Journal of the Optical Society of America A
OPTICS, IMAGE SCIENCE, AND VISION

Assessing the effects of dynamic luminance contrast noise masking on a color discrimination task

JOÃO M. M. LINHARES,[1,*] CATARINA A. R. JOÃO,[1] EVA D. G. SILVA,[1] VASCO M. N. DE ALMEIDA,[2] JORGE L. A. SANTOS,[2] LETICIA ÁLVARO,[3] AND SÉRGIO M. C. NASCIMENTO[1]

[1]Centre of Physics, Campus de Gualtar, University of Minho, 4710-057 Braga, Portugal
[2]Department of Physics, University of Beira Interior, 6201-001 Covilhã, Portugal
[3]Facultad de Psicología, Universidad Complutense de Madrid, 28883 Pozuelo de Alarcón, Spain
*Corresponding author: jlinhares@fisica.uminho.pt

Received 8 October 2015; revised 20 December 2015; accepted 22 December 2015; posted 23 December 2015 (Doc. ID 251582); published 5 February 2016

The aim of this work was to assess the influence of dynamic luminance contrast noise masking (LCNM) on color discrimination for color normal and anomalous trichromats. The stimulus was a colored target on a background presented on a calibrated CRT display. In the static LCNM condition, the background and target consisted of packed circles with variable size and static random luminance. In the dynamic LCNM condition, a 10 Hz square luminance signal was added to each circle. The phase of this signal was randomized across circles. Discrimination thresholds were estimated along 20 hue directions concurrent at the color of the background. Six observers with normal color vision, six deuteranomalous observers, and three protanomalous observers performed the test in both conditions. With dynamic LCNM, thresholds were significantly lower for anomalous observers but not for normal observers, suggesting a facilitation effect of the masking for anomalous trichromats.

OCIS codes: (330.0330) Vision, color, and visual optics; (330.1710) Color, measurement; (330.1720) Color vision.

http://dx.doi.org/10.1364/JOSAA.33.00A178

1. INTRODUCTION

Clinical assessment of color vision can be performed by a myriad of tests [1], including several that are run on a computer screen [2–5]. They determine the type and extent of the color vision impairment in inherited color vision deficiencies [6–8], diagnose and monitor clinical conditions in the eye, e.g., retinal conditions [9,10], eye conditions due to diabetes [9], and glaucoma [11], or assess the benefits of gene therapies [12], among others [13–15].

The wide use of such computerized techniques to perform clinical assessments might not be fully accepted as valid by the majority of the clinicians, due to the novelty of some of the tests and the lack of specificity and sensitivity of previous traditional color vision tests [16].

To ensure that discrimination of the target against the background is done only by chromatic cues and is not influenced by luminance [17], these tests require masking of some cues, which can be done by using random luminance contrast noise masking (LCNM) on random spatially located patches of different sizes. This eventually overcomes observers' individual differences in luminance and edge artifacts [2].

The use of dynamic LCNM reduces color discrimination for dichromats, in particular, protanopes and deuteranopes, by masking luminance contrast differences [18]. The role of luminance in chromatic discrimination tasks cannot be overlooked as luminance contrast increments in a color discrimination task using chromatic gratings improve color discrimination by adding luminance information to the chromatic task [19]. LCNM can also be used to test chromatic and luminance losses in certain pathologies [14] where observers were able to pass color screening tests but showed worse chromatic discrimination when dynamic LCNM was in use [14]. The impact of dynamic LCNM masking in anomalous trichromats is, however, still unknown.

This issue was addressed here by comparing the effect of LCNM masking on color discrimination thresholds. The color test was run on a computer screen. In the static LCNM condition, the background consisted of packed circles with variable size and random luminance on a uniform white area. In the dynamic LCNM condition, a 10 Hz square luminance signal was added to each circle. The phase of this signal was randomized across the circles. The target was a colored stimulus drawn

1084-7529/16/03A178-06$15/0$15.00 © 2016 Optical Society of America

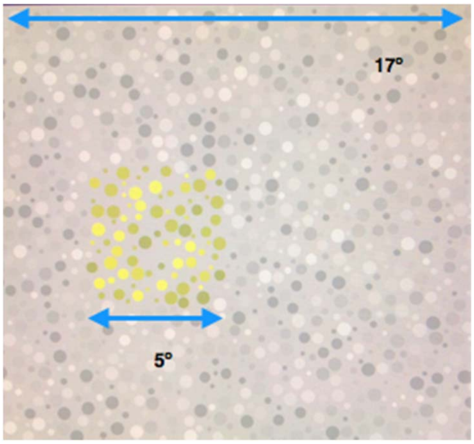

Fig. 1. Representation of the stimulus used in the experiment. The gray background represents the total area visible with packed disks of random luminance. The yellow area represents the test stimulus. The observers' task was to signal the position of the test stimulus, at the left or right side of the screen.

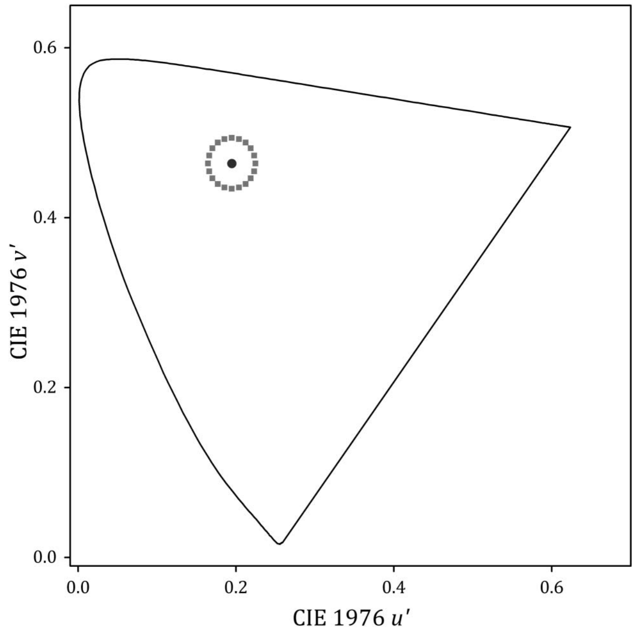

Fig. 2. Representation of the 20 hue directions tested (gray squares). Each is concurrent at the color of the background (dark gray circle).

on top of the background on the left or right side of the screen. Chromatic thresholds were estimated and compared across 20 hue directions concurrent at the background color.

2. METHODS

The color vision test used here was an in-house adaptation of the Universal Color Discrimination Test proposed elsewhere [4].

A. Apparatus

The test was run on a CRT color display (Sony–GDM F520, Sony Corporation, Tokyo, Japan) driven by a ViSaGe MKII system (Cambridge Research Systems, Kent, UK). The display screen was calibrated in color and luminance using a telespectroradiometer (SpectraColorimeter, Model PR-650, Photo Research Inc., Chatsworth, California, USA). The observers' distance to the computer screen was of 1 m, entailing a field of view of 17°.

B. Stimuli

The stimulus had three components and can be seen in Fig. 1. A uniform background of color (0.1947, 0.4639) in the CIE 1976 (u′, v′) UCS diagram [20] and 11 cd/m^2. The uniform area was packed with disks with variable size, occupying from 1% to 4% of the size of the total display area at random positions. Each disk had a random luminance ranging from 6 to 16 cd/m^2, with the same color as the white uniform area. The target appeared on top of the background, either on the left or on the right side of the screen, and can be seen in yellow in Fig. 1. The target area was located off center by 0.3° and fulfilled an area of 5° of visual angle. The color of the target circles was selected from 20 hue directions concurrent at the color of the background. Figure 2 represents the 20 hue directions as gray squares, the color of the background as the gray circle. Each hue could have a maximum distance from the background color of 0.03 in u′v′ 1976 UCS units. When required, the luminance of each disk changed randomly in the range of 6–16 cd/m^2 every 100 ms, resulting in a random dynamic LCNM of 10 Hz. This dynamic noise was added to the existing pattern of random luminance.

C. Observers

Fifteen observers performed the experiment. All observers were assessed, diagnosed, and characterized as normal color vision or color vision deficient (CVD) using the Farnsworth–Munsell 100 hue color vision test [1], the Oculus HMC anomaloscope [21], the Cambridge Color Test (CCT) [2] and the Color Assessment & Diagnosis (CAD) test [5].

Six observers were considered to have normal color vision. The remaining nine were characterized as CVD observers. The normal observers were three males and three females with an average age of 28 years (±10 years). The deuteranomalous observers were five males and one female with an average age of 32 years (±12 years). The protanomalous observers were two males and one female with an average age of 35 years (±9 years). All observers had normal ocular media and performed the test with their best-corrected vision. All observers had access to and signed a consent form where the experimental procedure was explained.

Figure 3 depicts the individual thresholds for all observers assessed using the CAD, the CCT, and the in-house software using the static LCNM condition. Data are for deuteranomalous (top row) and protanomalous (bottom row) observers. The first column represents averaged data across three repetitions of the test. The remaining data represents data from a single run of the CAD and the CCT tests. The data in the first two columns assume that Hue 1 matches a hue angle of 90° progressing counterclockwise. The testing protocol applied to the CCT test

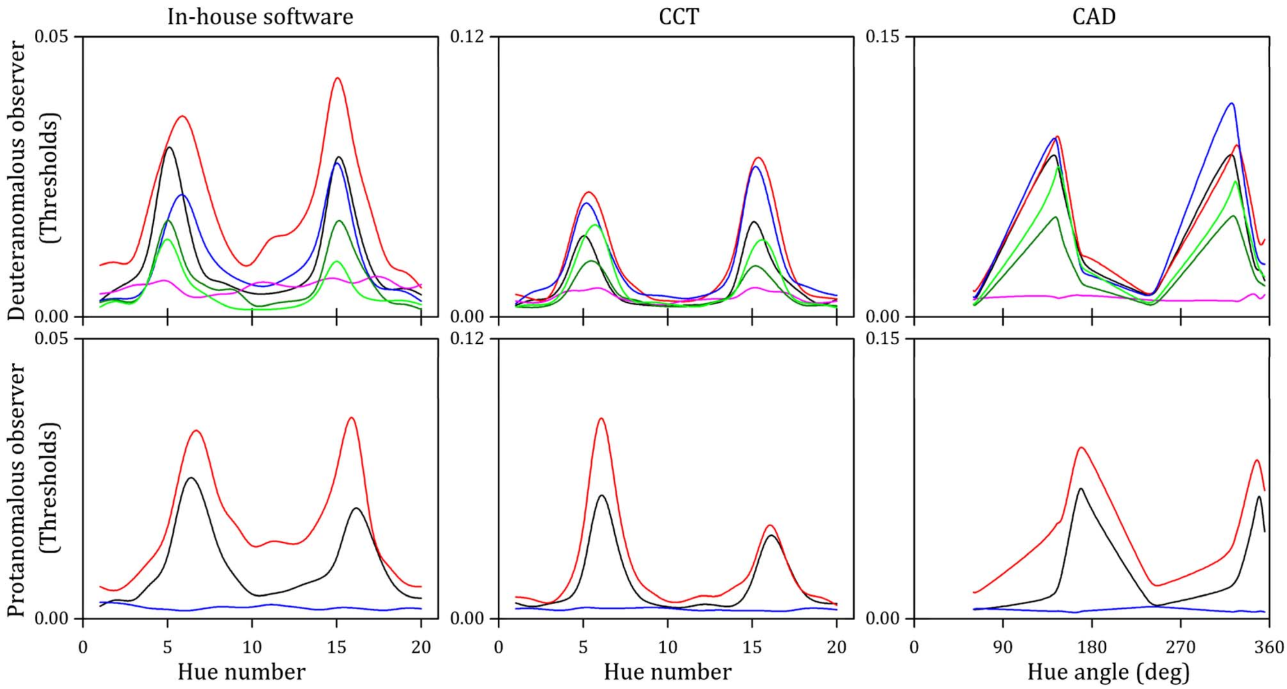

Fig. 3. Thresholds for deuteranomalous (top row) and protanomalous (bottom row) obtained from the in-house software with static LCNM (first column), the CAD system (middle column), and the CCT (last column). The first column represents averaged data across three repetitions of the test. The remaining data represents data from a single run of the CAD and the CCT tests. Data in columns 1 and 2 assume that Hue 1 matched a hue angle of 90° progressing counterclockwise.

assumed 20 vectors centered on (0.1947, 0.4639) in the CIE 1976 (u′, v′) space from 0° to 360° in 18° steps. The testing protocol applied to the CAD was the standard one, which assumed 16 vectors centered on (0.1947, 0.4639) in the CIE 1976 (u′, v′) space at the following angles: [60,64,140,145, 150,165,170,175,240,244,320,325,330,345,350,355] deg.

D. Procedure

In a two-alternative forced choice with a staircase procedure, the detection thresholds were estimated along each of the 20 hue directions. The observers' task was to signal the position of the target on the screen, either on the left or on the right side. The observer was instructed to freely gaze across the screen. Each observer performed three repetitions of the test under two different conditions. The first testing condition was with static random LCNM, and the second testing condition was with dynamic random LCNM. In each case, the background and the target were visible for 1 s. A pair of complementary hue directions was randomly selected. Of these, the first hue under testing was also randomly selected and presented as the target to its maximum saturation. The next stimulus was selected randomly from these 2 hues until both thresholds were obtained. The next pair of complementary hues was then randomly selected, until all the 20 hues were tested. The two testing conditions were done on different weeks, and the three repetitions of each testing condition were done on different days. To estimate the chromatic thresholds, only the last 15 answers (roughly four inversions) were used and averaged for each individual hue.

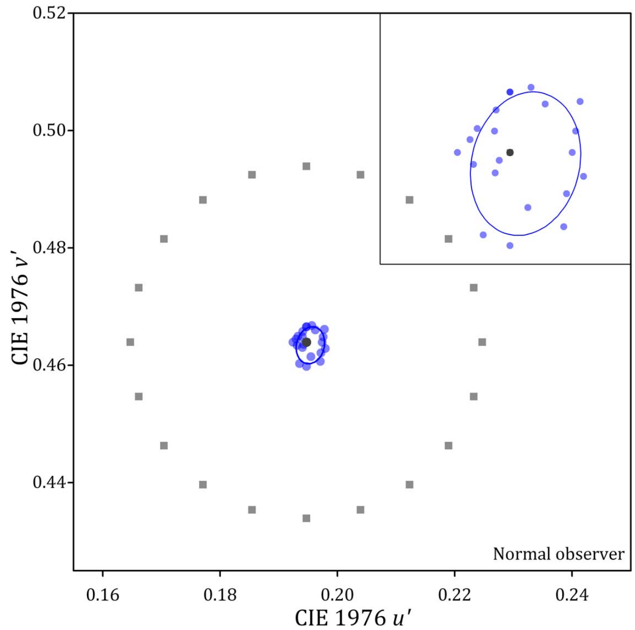

Fig. 4. Average thresholds (blue circles) for a normal observer with the static LCNM condition. Gray squares represent the hue directions under testing (with the central gray disk representing the color of the background). The blue line represents the fitted ellipse to the data points. The inset represents the same data, magnified for better visualization.

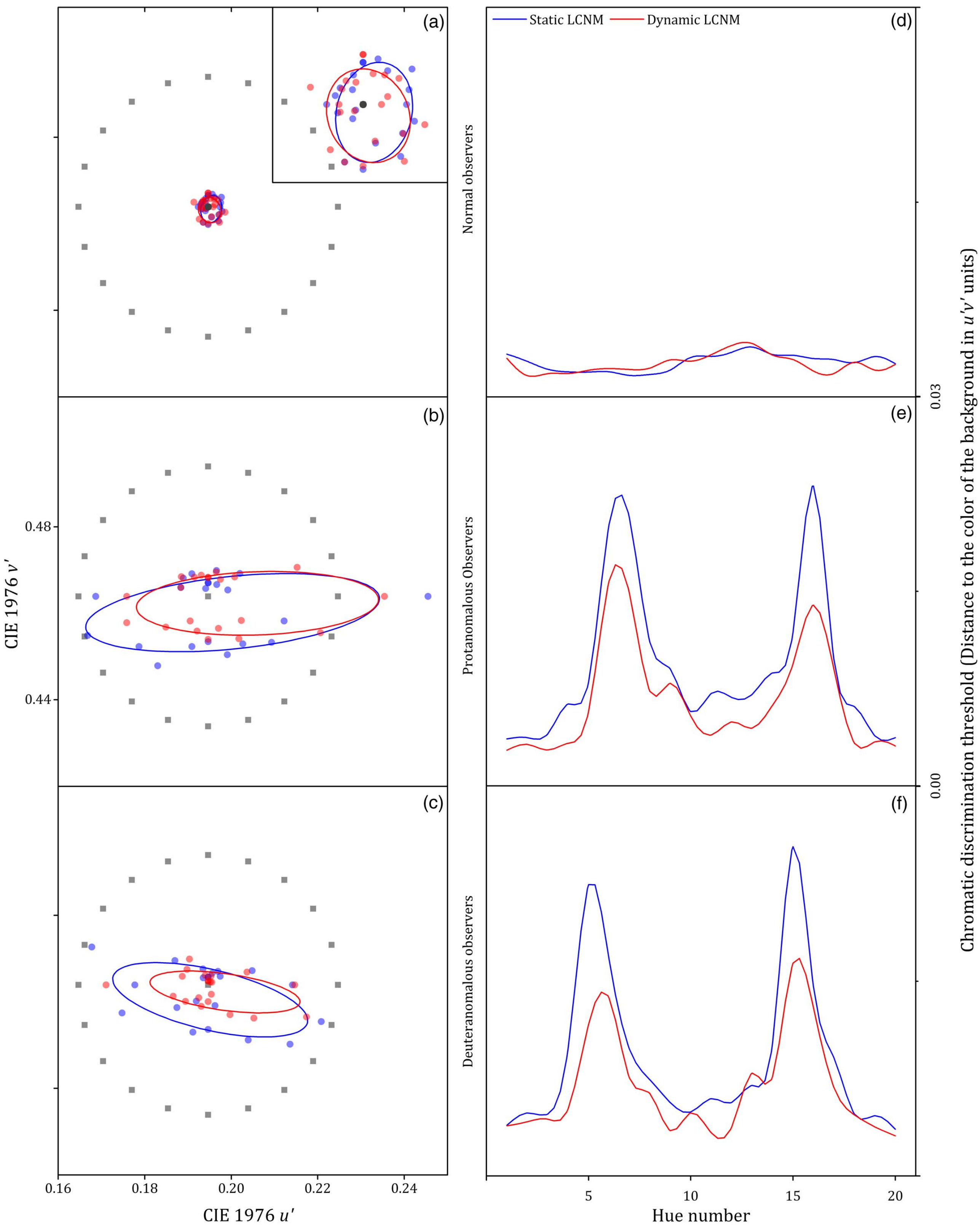

Fig. 5. (a)–(c) Represent the same data as Fig. 4 (blue for static LCNM condition) complemented with data obtained with the dynamic LCNM condition represented by red symbols and red line for all normal, protanomalous, and deuteranomalous observers, respectively. (d)–(f) Represent the distance of the threshold from the color of the background (the central gray point) for all 20 hue directions. Blue lines represent the static LCNM condition, and red lines represent the dynamic LCNM condition. Flat lines would represent an equidistance distance across the 20 hues. The two maxima for the anomalous observers [(e) and (f)] correspond to the major axis of the fitted ellipsis.

3. RESULTS

The blue circles in Fig. 4 represent average thresholds of three repetitions for the static LCNM condition for a normal color vision observer (the 20 hues under testing are represented as gray squares, with the central gray square being the color of the background). For better visualization, an ellipse was fitted to the data and is represented by a blue line. All ellipses were fitted to the data using an algorithm described elsewhere [22]. Figure 5(a) represents the same type of data as Fig. 4, showing averages across all observers and the data for the dynamic LCNM testing condition (red symbols and line). Figures 5(b) and 5(c) represent the same data as Fig. 5(a), but it is averaged across all protanomalous and deuteranomalous observers. In this figure, the enlargement of one of the axes of the ellipse is clearly visible, denoting higher thresholds than in the case of the normal observer. For better visualization and comparison, the Euclidean distance from each threshold to the color of the background (the central gray point) was estimated and plotted as a function of the hue direction. Hue 1 corresponded to the gray point in Fig. 2 at 12 o'clock (or 90º), progressing counterclockwise. Figures 5(d)–5(f) represent this data. The blue lines represent the data for the static LCNM condition, and the red lines represent the dynamic LCNM condition. Flat lines would represent an equidistance to the color of the background across the 20 hues, which was roughly the case of the normal observer condition—the lines are almost flat [Fig. 5(d)]. For deuteranomalous and protanomalous observers [Figs. 5(e) and 5(f), respectively], the two maxima correspond to the ellipse-fitted elongated arms and indicate poorer discriminability.

Figure 6 represents the average results for the two testing conditions for normal, deuteranomalous, and protanomalous observers, whose numerical data are represented in Table 1. The blue bars represent the static and red bars the dynamic LCNM conditions. Deuteranomalous and protanomalous observers revealed significant differences between the two testing conditions ($p < 0.001$), while normal observers did not. The discrimination thresholds were lower in the dynamic LCNM condition, indicating a better chromatic discrimination. The error bars in Fig. 6 and the error figures in Table 1 represent the standard error of the mean. A Wilcoxon signed-rank test for two dependent samples was performed using IBM SPSS Statistics v21 (IBM Corporation, New York, USA). The normality of the data was tested using the Shapiro–Wilk test in IBM SPSS Statistics v21, which revealed non-normal data across observers ($p < 0.05$).

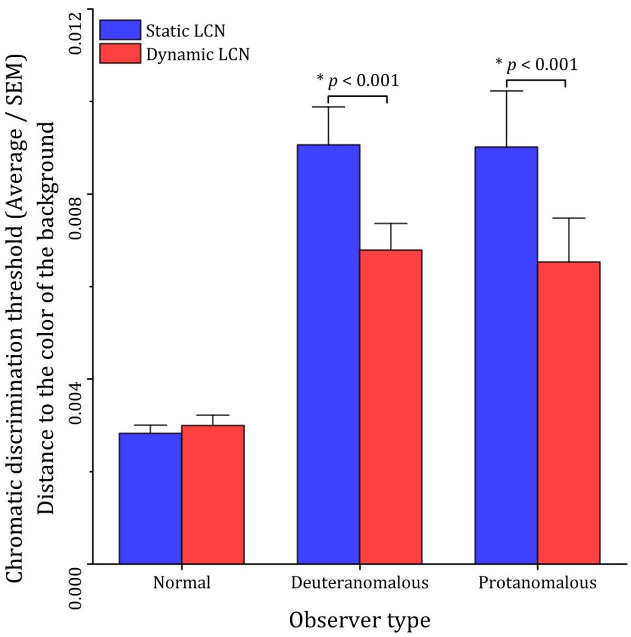

Fig. 6. Average results of the discrimination thresholds for the two testing conditions for normal and anomalous observers. Blue bars represent the static and red bars the dynamic LCNM conditions. Only in the anomalous observer's situation was there a significant difference between the two testing conditions ($p < 0.001$). Error bars represent the standard error of the mean.

Table 1. Average Results of the Discrimination Thresholds for the Two Testing Conditions for Normal and Anomalous Observers[a]

	Luminance Contrast Noise [Mean (± SEM)]	
Observer Type	Static	Dynamic
Normal	2.8E-3 (±1.7E-4)	3.0E-3 (±2.2E-4)
Deuteranomalous*	9.1E-3 (±8.2E-4)	6.8E-3 (±5.8E-4)
Protanomalous*	9.0E-3 (±1.2E-3)	6.5E-3 (±9.5E-4)

[a]Only anomalous observers presented a significant difference between the two testing conditions (signaled by * for $p < 0.001$). Errors represent the standard error of the mean (SEM). The numerical data is plotted in Fig. 6.

4. CONCLUSION AND DISCUSSION

In this work, a computer screen test developed in-house was used to assess the effect of dynamic LCNM masking on the color discrimination of normal and anomalous trichromats. No statistical difference between static and dynamic noise was found for normal observers. For anomalous trichromats, however, dynamic LCNM clearly improved chromatic discrimination.

The effect of the dynamic LCNM on normal observers was described elsewhere [18,23] and proved to mask the luminance detection contrast signal as successfully as static LCNM. For dichromats, however, dynamic LCNM produced higher thresholds than static LCNM [18]. Here, we replicated the results for normal observers. Moreover, we found that for the stimulus conditions employed in our study, the presence of dynamic LCNM yields lower thresholds in deuteranomalous and protanomalous subjects when compared to static LCNM [18].

Individual variations in the optical density, cone-photopigment spectra, and cone weightings affect individual perceptions of color and have an impact on chromatic thresholds [24]. Nevertheless, in this work, the comparison is made intra-observer, so such effects may be ruled out.

Despite the individual variations for anomalous observers, the effect is present in all but one: all protanomalous observers and five out of the six deuteranomalous observers presented the same tendency of higher thresholds with the static LCNM condition.

The fact that the target stimulus was 5° in eccentricity, where the luminance function and other properties are different from the central region [2,25–30], may be a factor to consider. Other studies that compared the static with the dynamic LCNM conditions used a stimulus of 4° centered on the background [18], which is a smaller visual angle than the one used here.

The frequency selected for the dynamic LCNM might also impact the final result. There is evidence that for normal and dichromats at different frequencies [7,25], the test stimulus will influence the perceived luminance and chromaticity. The selected frequency used here might stimulate cells in the M pathway which are not dependent on the red–green color impairment and favor different post-receptor mechanisms on anomalous trichromats due to a possible affected L-M opponency mechanism leading to better chromatic discrimination [7,31,32]. This might also be true depending on the type of noise used, as different types of noise, and its temporal and spatial frequencies, will have different results on the spatial contrast sensitivity [32–34].

Funding. Centro de Física of Minho University; Departamento de Física of University of Beira Interior; FEDER through the COMPETE Program; Foundation for Science and Technology (FCT) (PTDC/MHC-PCN/4731/2012).

Acknowledgment. This work was supported by the Departamento de Física of University of Beira Interior, by the Centro de Física of Minho University, by FEDER through the COMPETE Program, and by the Portuguese Foundation for Science and Technology (FCT) in the framework of the project PTDC/MHC-PCN/4731/2012.

REFERENCES

1. B. L. Cole, "Assessment of inherited colour vision defects in clinical practice," Clin. Exp. Optom. **90**, 157–175 (2007).
2. B. C. Regan, J. P. Reffin, and J. D. Mollon, "Luminance noise and the rapid determination of discrimination ellipses in colour deficiency," Vis. Res. **34**, 1279–1299 (1994).
3. T. Squire, M. Rodriguez-Carmona, A. Evans, and J. Barbur, "Color vision tests for aviation: comparison of the anomaloscope and three lantern types," Aviat. Space Environ. Med. **76**, 421–429 (2005).
4. C. Ripamonti, S. Kalwarowsky, and M. Nardini, "A novel colour discrimination test suitable for low vision observers," in *12th International AIC Congress* (International Color Association, 2014), pp. 1–4.
5. J. Barbur, M. Rodriguez-Carmona, S. Evans, and N. Milburn, "Minimum color vision requirements for professional flight crew, part 3: recommendations for new color vision standards," CAA Paper 2009/04 (2009).
6. B. L. Cole, "The handicap of abnormal colour vision," Clin. Exp. Optom. **87**, 258–275 (2004).
7. L. T. Sharpe, E. de Luca, T. Hansen, H. Jägle, and K. R. Gegenfurtner, "Advantages and disadvantages of human dichromacy," J. Vis. **6**, 213–223 (2006).
8. J. Birch, *Diagnosis of Defective Colour Vision*, 2nd ed. (Butterworth-Heinemann, 2001).
9. M. O'Neill-Biba, S. Sivaprasad, M. Rodriguez-Carmona, J. E. Wolf, and J. L. Barbur, "Loss of chromatic sensitivity in AMD and diabetes: a comparative study," Ophthalmic. Physiol. Opt. **30**, 705–716 (2010).
10. S. H. Campos, V. Forjaz, L. R. Kozak, E. Silva, and M. Castelo-Branco, "Quantitative phenotyping of chromatic dysfunction in best macular dystrophy," Arch. Ophthalmol. **123**, 944–949 (2005).
11. M. Castelo-Branco, P. Faria, V. Forjaz, L. R. Kozak, and H. Azevedo, "Simultaneous comparison of relative damage to chromatic pathways in ocular hypertension and glaucoma: correlation with clinical measures," Invest. Ophthalmol. Visual Sci. **45**, 499–505 (2004).
12. K. Mancuso, W. W. Hauswirth, Q. Li, T. B. Connor, J. A. Kuchenbecker, M. C. Mauck, J. Neitz, and M. Neitz, "Gene therapy for red–green colour blindness in adult primates," Nature **461**, 784–787 (2009).
13. M. F. Silva, P. Faria, F. S. Regateiro, V. Forjaz, C. Januário, A. Freire, and M. Castelo-Branco, "Independent patterns of damage within magno-, parvo- and koniocellular pathways in Parkinson's disease," Brain **128**, 2260–2271 (2005).
14. P. Flanagan and A. J. Zele, "Chromatic and luminance losses with multiple sclerosis and optic neuritis measured using dynamic random luminance contrast noise," Ophthalmic. Physiol. Opt. **24**, 225–233 (2004).
15. S. J. Hickman, N. Raoof, R. J. McLean, and I. Gottlob, "Vision and multiple sclerosis," Mult. Scler. Relat. Disord. **3**, 3–16 (2014).
16. M. Rodgers, R. Hodges, J. Hawkins, W. Hollingworth, S. Duffy, M. McKibbin, M. Mansfield, R. Harbord, J. Sterne, P. Glasziou, P. Whiting, and M. Westwood, "Colour vision testing for diabetic retinopathy: a systematic review of diagnostic accuracy and economic evaluation," NIHR Health Technol. Assess. Program. **13**, 1–160 (2009).
17. A. Yebra, J. Garcia, J. Nieves, and J. Romero, "Chromatic discrimination in relation to luminance level," Color Res. Appl. **26**, 123–131 (2001).
18. J. Birch, J. L. Barbur, and A. J. Harlow, "New method based on random luminance masking for measuring isochromatic zones using high-resolution color displays," Ophthalmic. Physiol. Opt. **12**, 133–136 (1992).
19. R. L. Hilz, G. Huppmann, and C. R. Cavonius, "Influence of luminance contrast on hue discrimination," J. Opt. Soc. Am. **64**, 763–766 (1974).
20. CIE, "Colorimetry," CIE **15**, 1–82 (2005).
21. G. Jordan and J. D. Mollon, "The Nagel anomaloscope and seasonal variation of colour vision," Nature **363**, 546–549 (1993).
22. A. Fitzgibbon, M. Pilu, and R. B. Fisher, "Direct least square fitting of ellipses," IEEE Trans. Pattern Anal. Mach. Intell. **21**, 476–480 (1999).
23. J. L. Barbur, ""Double-blindsight" revealed through the processing of color and luminance contrast defined motion signals," Prog. Brain Res. **144**, 243–259 (2004).
24. V. Smith and J. Pokorny, "Chromatic-discrimination axes, CRT phosphor spectra, and individual variation in color-vision," J. Opt. Soc. Am. A **12**, 27–35 (1995).
25. W. H. Swanson, T. Ueno, V. C. Smith, and J. Pokorny, "Temporal-modulation sensitivity and pulse-detection thresholds for chromatic and luminance perturbations," J. Opt. Soc. Am. A **4**, 1992–2005 (1987).
26. D. H. Foster, R. S. Snelgar, and J. R. Heron, "Nonselective losses in foveal chromatic and luminance sensitivity in multiple sclerosis," Invest. Ophthalmol. Visual Sci. **26**, 1431–1441 (1985).
27. H. Strasburger, I. Rentschler, and M. Juttner, "Peripheral vision and pattern recognition: a review," J. Vis. **11**(5):13, 1–82 (2011).
28. M. P. S. To, I. D. Gilchrist, T. Troscianko, and D. J. Tolhurst, "Discrimination of natural scenes in central and peripheral vision," Vis. Res. **51**, 1686–1698 (2011).
29. S. G. Solomon, B. B. Lee, A. J. R. White, L. Rüttiger, and P. R. Martin, "Chromatic organization of ganglion cell receptive fields in the peripheral retina," J. Neurosci. **25**, 4527–4539 (2005).
30. B. Stabell and U. Stabell, "Spectral sensitivity in the far peripheral retina," J. Opt. Soc. Am. **70**, 959–963 (1980).
31. S. J. Dain and P. E. King-Smith, "Visual thresholds in dichromats and normals; the importance of post-receptoral processes," Vis. Res. **21**, 573–580 (1981).
32. K. R. Gegenfurtner and D. C. Kiper, "Contrast detection in luminance and chromatic noise," J. Opt. Soc. Am. A **9**, 1880–1888 (1992).
33. J. J. Mcanany and K. R. Alexander, "Spatial contrast sensitivity in dynamic and static additive luminance noise," Vis. Res. **50**, 1957–1965 (2010).
34. G. Chen, F. Hou, F.-F. Yan, P. Zhang, J. Xi, Y. Zhou, Z.-L. Lu, and C.-B. Huang, "Noise provides new insights on contrast sensitivity function," PLoS ONE **9**, e90579 (2014).